SCIENTIFIC PAPER
Published: September 30, 2025
https://doi.org/10.13167/2025.31.8

Effect of varying soil conditions on soil-structure interaction in berthing structures: A case study using modelling approach

Namratha Sasikumar[1]✉, Ilamainathan Natarajan[2] and Joanna Philip Saratha[1]

[1] *Hindustan Institute of Technology & Sciencet,603103, Chennai, India*

[2] *Worley India Pvt. Limited, Marine and Coastal, 600094, Chennai, India*

Corresponding author:
Namratha Sasikumar

Received:
March 20, 2024

Revised:
April 6, 2025

Accepted:
April 23, 2025

Published:
September 30, 2025

Citation:
Sasikumar, N.; Natarajan, I.; Saratha, J. P.
Effect of varying soil conditions on soil-structure interaction in berthing structures: A case study using modelling approach.
Advances in Civil and Architectural Engineering,
2025, 16 (31), pp. 130-145.
https://doi.org/10.13167/2025.31.8

ADVANCES IN CIVIL AND ARCHITECTURAL ENGINEERING (ISSN 2975-3848)

Faculty of Civil Engineering and Architecture Osijek
Josip Juraj Strossmayer University of Osijek
Vladimira Preloga 3
31000 Osijek
CROATIA

Abstract:
The substructure of a berthing structure with a deep draft presents significant financial challenges. This research offers valuable perspectives on minimizing substructure expenses for a berthing structure by leveraging the Indian Standard (IS) code for deep draft berthing structures in the early project phase for the prompt creation of the bill of quantities. The focus is on achieving efficient results, while adhering to the IS approach, thus avoiding time-consuming analyses. Different analyses of soil-structure interaction, including those based on the Indian Standard (IS) code, Fixity method, linear analysis, and non-linear analysis approaches were conducted utilising actual field soil parameters. Three distinct sites, predominantly comprised of sand (Chennai port), clay (Cochin port), and rock (Bhavanapadu port) were chosen for conducting optimised analyses. The analysis methodology involved creating four models for each site, along with IS Standard theoretical approaches. The models of the berthing structures were developed using STAAD Pro software, with detailed load calculations incorporated into the analysis. Results were presented as percentage variations in bending moments, shear force, and deflection obtained by different methods, revealing that the IS approach is comparatively non-conservative.

Keywords:
IS Code; Fixity Linear and Non-Linear; STADD Pro

1 Introduction

Berthing structures are erected in ports and harbours to accommodate the docking and mooring of vessels, facilitate the seamless loading and unloading of cargo, and provide designated areas for passengers to board and disembark from vessels. Owing to continuous economic growth and global trends, major ports in India are increasing the draft depth of berthing structures to match their cargo profiles. Historically, major ports have featured relatively shallow draft depths of approximately 7 m in older ports and up to 20 m in newer ports in both channels and berths. Considering these stipulations, this study is conducted to examine the behaviour of berthing structures under various soil conditions with deep draft depths. For this purpose, very deep draft vessels of the Suezmax class with a displacement tonnage of 208000, length of 400 m, breadth of 50 m, and a maximum draft of 20,1 m were chosen [1]. Jayasree et al. [2] conducted a study on conservatism in the analysis of laterally loaded piles (bridges) as per Indian Standards (IS) and Vesic's equation. Utilising field data collection and STAAD Pro modelling, their research revealed that IS methods exhibit economic inefficiency and excessive conservatism compared with theoretical models. Kumar et al. [3] examined various factors influencing the analysis and design of berthing structures. Their investigation centred on a prospective berthing structure slated for Belekeri port, leveraging data gathered from the Karwar region. Using these data, a structure was planned and analysed using STAAD Pro V8i software. Design variations across five distinct scenarios, culminating in insights into the economic and safety implications associated with each configuration were assessed.

Priyanka et al. [4] examined the application of IS codes to analyse the behaviour of jetty structures under various marine loads and load combinations. They discussed the modelling and design considerations for all seismic zones in India, and highlighted the sensitivity of the structure to different loads. Factors such as the bedrock nature and pile embedment depth were deemed crucial for berthing force calculation. In seismic zones II and III, the berthing force governed the design, whereas in zones IV and V, seismic force assumed precedence. Himesh et al. [5] explored the importance of jetties for cost-effective transportation of goods and materials. The challenges posed by marine loads such as currents, waves, berthing, and mooring forces were addressed. They calculated and applied such forces for structural analysis to accurately comprehend their effects. Wind forces were applied above the mean sea level, whereas wave and current forces were assigned as nodal and uniformly varying loads, respectively, below the average mean sea level. Despite their unpredictable nature, analytical simulations have been proposed to depict the behaviour of jetty structures under the influence of wave and current forces. Rajkumar et al. [6] investigated the performance of diaphragm walls in berthing structures by examining four models with various configurations of diaphragm walls and supporting piles. Their findings suggested a preference for diaphragm walls positioned on the seaside, and the addition of a raker pile improved the efficiency, particularly in areas with weak soil conditions on the land side. Chaudhari et al. [7] reported that ports and harbours play a crucial role in facilitating cost-effective transportation of goods and public accessibility, thereby serving as a cornerstone of a nation's economic progress. Jetties, which are essential for transporting large volumes of goods and fuel, provide economical access to waterways. Their study outlined the calculation of forces on jetty structures under additional marine loads, following the guidelines set by the IS 4651 standards. There is a scarcity of literature on cost-effective design methodologies for berthing structures, particularly in terms of establishing a bill of quantities at the inception of the project. This study aims to address this gap by analysing berthing structures under diverse soil conditions, including sand, clay, and rock, using real-field soil parameters. To study the behaviour of piles under significant lateral forces from vessels and environmental loads, three sites were characterised predominantly by sand (Chennai port), clay (Cochin port), and rock (Bhavanapadu port).

Traditionally, offshore substructures are built using cast-in-situ concrete or steel piles accompanied by suitable deck systems. Owing to the substantial diameters and lengths of these piles compared with conventional structures and the associated high construction costs, this study explores various analyses to minimise the expenses of construction materials such as steel, concrete, and pile diameters. These analyses include methods based on IS codes, the Fixity method, and linear, non-linear analyses of soil-structure interactions. Furthermore, the bending moments experienced by berthing structures from different analyses were compared with the IS standard approach, and suggestions were provided to possibly reduce bending moments when using the IS approach, thus avoiding additional time-consuming analyses.

2 Site Condition

It is essential to analyse the prevailing environmental aspects of a project site to better understand the site, which can help in the development and modification of the structure. Hence, the overall meteorological parameters, oceanographic conditions, and geotechnical investigations for the ports of Chennai [8], Cochin [9; 10], and Bhavanapadu [11] were considered. To handle the Suezmax vessels, the berthing structure dredge level was kept at -22,10 m CD (Chart Datum), and the corresponding tide, wave, current, and wind forces were considered for the appropriate site. The seismicity [12] of the selected zone is under the zone III category with moderate-risk seismic intensity. The unit weight of the soil and c-ϕ values were selected in accordance with the information provided in the geotechnical report [8; 10; 11]. The Young's modulus [13] of the soil was chosen based on the soil parameters and correlated with the corresponding "N" values. The type of soil used for the Chennai port was medium dense to dense sand; for the Cochin port, it was greyish silty clay with fine particles; and hard rock at Bhavanapadu port. The elevation of each soil layer was specified based on the chart datum. The geotechnical data including the selected unit weight, c-ϕ values and Young's modulus of soil are presented in Table 1.

Table 1. Geotechnical data

Sl, No,	**Elevation w,r,t CD** (m)		**Type of Soil**	**"N" Value**	**ϕ °**	γ_{sat} (kN/m^3)	γ_{sub} (kN/m^3)	**C** (kN/m^2)	**Young's modulus Es** (kN/m^2)
Chennai Port (Sand)									
1	4,0	0,5	Filled up Soil	---	---	---	---	---	---
2	0,5	−1,5	Very Loose Sand	4	18	16,0	5,975	---	4750
3	−1,5	−10,5	Dense to Very Dense Sand	62	35	18,5	8,475	---	12500
4	−10,5	−11,5	Hard Rock	> 50	---	21,0	10,975	500	3000000
5	−11,5	−27,5	Medium Dense to Dense	27	33	18,5	8,475	---	10500
6	−27,5	−45,0	Very Dense Sand	> 50	36	19,0	8,975	---	16250
Cochin Port (Clay)									
1	−6,0	−12,0	Very loose silty clay with seashells	1	---	16	5,975	12,5	7500
2	−12,0	−20,0	Blackish silty clay with seashells	12	---	20	9,975	65	32500
3	−20,0	−34,5	Greyish silty clay with fine particles	35	---	21	10,975	200	75000
4	−34,5	−44,0	Silty clay in greenish grey	40	---	21	10,975	200	75000
5	−44,0	−45,0	Blackish silty clay with fine particles	50	---	22	11,975	200	75000

Bhavanapdu Port (Rock)									
1	0,0	−2,0	Medium dense silty sand	20	31	18	7,975	---	8750
2	−2,0	−3,5	Dense silty Sand	35	33	18,5	8,475	---	12500
3	−3,5	−6,0	Very dense Sand	50	35	19	8,975	---	20000
4	−6,0	−7,5	Medium dense silty sand	19	31	18	7,975	---	8500
5	−7,5	−9,0	Loose silty Sand	4	20	16,5	6,475	---	4750
6	−9,0	−12,0	stiff to very stiff clay	18	---	18	7,975	70	35000
7	−12,0	−15,0	Medium dense sand	18	31	18	7,975	---	8250
8	−15,0	−19,5	Dense Sand	40	35	18,5	8,475	---	13750
9	−19,5	−21,0	Medium dense sand	75	37	18	7,975	---	10000
10	−21,0	−22,5	Weak rock	50	36	19	8,975	---	35000
11	−22,5	−45,0	Hard rock	>100	38	22	11,975	---	3000000

3 Structural system and design considerations

3.1 Structural system

The berthing structure was 460 m long and 35 metres wide [14]. The entire length of the berthing structure was separated into four units and expanded joints were provided every 115 m. In this study, the open piled structure type of berth was considered at −22,10 CD m water depth. The berth deck level was +6 m CD (representing height above the Chart Datum). The transverse pile spacing (Girds A, B, C, D, and E) was 8 m, and the longitudinal pile spacing was 7 m (16 bent). A 1500 mm pile diameter was maintained. The main beams were arranged transversely, whereas the crane and rectangular beams were arranged longitudinally to provide structural framing. The primary beams provided support for the slabs. The primary beam was set to a depth of 2000 mm and a width of 1600 mm. The beam's longitudinal dimensions were 1600 mm width and 1800 mm depth. A slab with a thickness of 500 mm was used. The same structural framing was used for various soil scenarios. In the IS approach, the deflection, bending moment, and shear force values were estimated using the theoretical relationship provided in IS 2911 Part I, Section II [15]. For the Fixity method, linear analysis, and non-linear analysis, the structural framing was represented as a three-dimensional frame in STAAD Pro, encompassing the pile, beam, and slab, each with their respective support conditions. The entire structure was simulated as a single unit. The pile, beam, and slab elements were modelled using the pertinent properties of reinforced concrete. A typical model of a berthing structure is depicted in Figure 1.

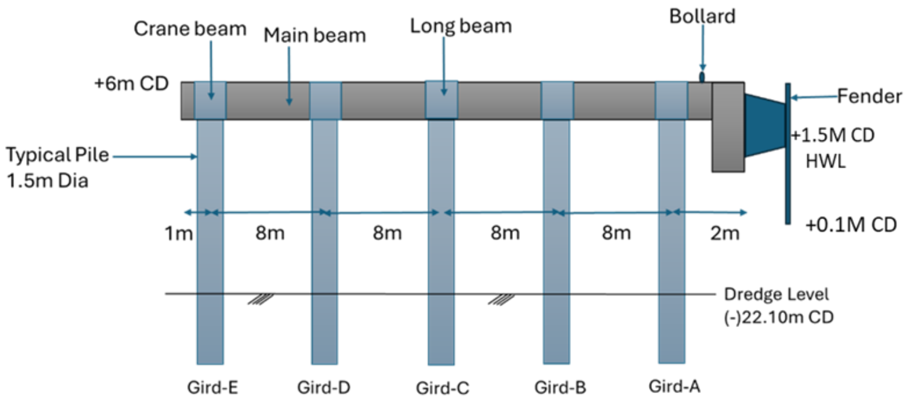

Figure 1. Typical cross section of a berthing structure

3.2 Design considerations

3.2.1 General

The operational lifespan of the berthing structure was considered to be 50 years, the design dredge level was kept at −22,10 m CD [14], the clear cover [16] to the outermost reinforcement of the pile was considered to be 75 mm, and for the superstructure, it was 50 mm.

3.2.2 Material properties

The selected compressive strength of the concrete for both the substructure and superstructure was 40 N/mm² [16], and the yield strength of the reinforcement was set as 500 N/mm² (Fe500).

3.2.3 Tidal data

The tidal data for the three site conditions is presented as follows: Highest High-Water Spring: +1,5 m CD for Chennai port [8], +1,2 m CD for Cochin port [9] and +1,7 m CD for Bhavanapadu port [11]. Lowest low-water spring: +0,1 m CD for Chennai port, +0,3 m CD for the Cochin and Bhavanapadu ports.

3.3 Loads

Berthing structures experience forces such as dead loads, live loads, berthing and mooring forces, wave and current forces, seismic forces, crane forces, stacking live loads, wind forces, and forces owing to temperature and shrinkage. They are subjected to significant vertical and lateral forces that have a major role in determining the pile diameter and material requirements. Vertical forces mainly result from crane operations during the loading and unloading of containers and cargo. Hence, vertical forces are developed by the self-weights of the superstructure and crane, operational container weights, and container stacking. When a crane loads and unloads goods from the ship to the shore, a large axial compression load is imposed on the front row of the crane piles. Similarly, for goods loaded from the shore to the ship, a large axial compression load is transferred through the land-side crane piles. The length of the pile is primarily based on the maximum axial compression load and draft requirements. Large lateral forces are mobilised through the berthing and mooring of vessels, seismic forces, and wave and current forces. When vessels are berthed, the entire lateral force is transferred through the piles according to their stiffness ratios. Typically, piles at the outermost positions or near expansion joints, if equipped with fenders, bear the berthing force and are subjected to the maximum design forces and loads. During the berthing process, certain front-row piles are under axial tension, whereas land-side piles experience axial compression. Similarly, when vessels are moored, this dynamic is reversed. The lateral force determines the point of fixity according to the ground conditions and influences the length of the piles, which in turn determines the bending moment and deflection magnitude.

3.3.1 Wave and current

The wave and current data for the three site conditions were established as follows: the operating wave height was 2,5 m [8; 9; 11] and the corresponding time period was 10 s. Additionally, a current speed of 1,5 m/s [8; 9; 11] was considered for all sites because the structure would be located in the open sea. The forces acting on the structure were determined using Equations 1 and 2:

$$F_{drag} = 1/2 C_d \rho D u^2 \tag{1}$$

$$F_{inertia} = C_m \rho (\pi D^2/4) a \tag{2}$$

where C_d is the drag coefficient, ρ is the density of sea water, D is the pile diameter, u is the water particle velocity, C_m is the inertia coefficient, and a is the water particle acceleration.

The wave forces for the 1500 mm piles were calculated in accordance with IS 4651 Part-III [3], considering the data provided above. The determined wave force at the surface was 4,26 kN/m and that at the seabed was 2,67 kN/m.

3.3.2 Wind data

The wind forces on the structures were calculated according to IS 875, Part 3 [11]. The basic wind speed under these operating conditions was 20 m/s [1]. The forces acting on the structure were determined using Equation 3:

$$V_z = V_b \, k_1 \, k_2 \, k_3 \, k_4 \tag{3}$$

where V_z is the design wind speed at a height z (m/s), k_1 is the probability factor (risk coefficient), k_2 is the terrain roughness and height factor, k_3 is the topography factor, and k_4 is the importance factor of the cyclonic region. The calculated wind forces on the piles, beams, and slabs were 0,44 kN/m, 0,56 kN/m, and 0,16 kN/m, respectively.

3.3.3 Dead load

The dead load of the structural components, including the piles, beams, and slabs, was estimated based on the respective material unit weights and applied within the model. These dead loads contribute to the overall structural analysis and design considerations [17; 18]. Marine growth of 50 mm thickness (on radius) on the circumference of the piles was considered, while assessing the wave/current forces, as per IS 4651 [16].

3.3.4 Live load

For berth analysis, the live loads considered according to IS 4651 [1] were as follows: 30 kN/m² on the berth where the crane did not occupy the area, and 10 kN/m² under the crane during operation.

3.3.5 Crane load

The rail-mounted gantry crane comprised 12 wheels per corner, and the centre-to-centre rail distance was 30 m. The considered crane loads are listed in Table 2.

Table 2. Crane data

Description	**Land Side** (kN)		**Seaside** (kN)	
Vertical load	6360	6360	2280	2280
Per Wheel	530	530	190	190

3.3.6 Berthing force

Upon impact with a berth, the approaching vessel imparts a horizontal force on the berth. The intensity of this force depends on the kinetic energy absorbed by the fendering system [19]. The design process for the berthing structure entails determining the reaction force. This was achieved by selecting the deflection-reaction diagrams corresponding to the preferred fendering system. The design berthing energy was calculated under moderate conditions in accordance with IS 4651 [1] based on the parameters stated below. It was assumed that the designed vessels under fully loaded conditions berthed at an angular approach of a maximum of 10° with an approach velocity. The considered approach velocity was 0,15 m/s, with the friction force set at 0,20 times the reaction of the fender, serving as the longitudinal force. The data of the selected design vessels are listed in Table 3.

Table 3. Vessel data

Vessel Size		**Length** (m)	**Beam** (m)	**Draught- Loaded Condition** (m)
(DWT)	**(DT)**			
160000	208000	400	50	20,1

The berthing force was determined using Equation 4:

$$E=W_D V^2/2g\, C_m\, C_e\, C_s \quad (4)$$

where W_D is the displacement tonnage (DT) of the vessel (in tons), V is the velocity of the vessel (m/s), g is the acceleration due to gravity (ms^{-2}), C_m, C_e, and C_s are the mass, eccentricity, and softness coefficients, respectively.
In order to absorb the design berthing energy of 3757 kNm, a suitable super cone fender (SCN 2000 E1.8) was selected. The corresponding reaction from the supercone fender was 3292 kN [16] and was applied to the model. Additionally, a longitudinal force of 670 kN was applied to account for the specific forces and interactions involved in the berthing scenario.

3.3.7 Mooring force

Mooring loads are commonly referred to as lateral forces and are generated by mooring lines as they pull the ship towards or along the dock or provide stabilisation against the forces of wind or tides. The mooring load was determined based on the displacement of the designed vessel. In adherence to IS 4651 Part III:2020 [1], a bollard capacity of 200 T was selected and applied to the model to accommodate the mooring loads effectively.

3.3.8 Seismic force

The seismic loads were calculated using IS 1893 (Part 1:2016) [12], and the design horizontal seismic coefficient Ah for the structure was determined using Eqation 5:

$$A_h = \left(\frac{Z}{2}\right)\left(\frac{S_a}{g}\right)\left(\frac{I}{R}\right) \quad (5)$$

For seismic zone III, the zone factor Z is 0,16; and the average response acceleration coefficient S_a/g depends on the time period of the structure. The importance factor I = 1,5 and response reduction factor R = 3. The time period of the structure was evaluated by STAAD analysis considering *dead load + super imposed load + 50 % live load*.

3.3.9 Load combination and safety factors

The load combination for the berthing structure was formulated in accordance with IS: 4651-Part [16]. Considering the aforementioned loads, it was observed that the berthing force contributed more significantly to the lateral force than the mooring and seismic forces. As a result, the analysis considered only the berthing load combination, and it was: *1,0 dead load + 1,0 live load + 1,1 crane load + 1,0 wave and current force + 1,0 berthing force*. The seismic and mooring load combinations were neglected because the berthing was the governing force.

4 Analysis methodology

4.1 IS 2911 (Part 1/Sec 2)-2010 approach

The ultimate resistance of a vertical pile to lateral loads and the corresponding deflection with increase in load to the ultimate value involve intricate interactions between a semi-rigid structural element and soil that exhibits both elastic and plastic deformation. The failure mechanisms differ between an infinitely long pile and a short rigid pile, and further variations occur under restrained and unrestrained pile head conditions [15]. Owing to the complexity of this issue, an approximate solution, which is generally sufficient in most cases, is presented. It is determined whether the pile would exhibit the behaviour of a short rigid unit or an infinitely long flexible member. This value is determined by computing the stiffness factor (R or T) for a specific combination of piles and soil. Once the stiffness factor is determined, the criteria for behaviour (short rigid pile or long elastic pile) are related to the embedded length (L) of the pile. The depth from the ground surface to the point of virtual fixity is then calculated and utilised in conventional elastic analysis to estimate the lateral deflection and bending moment. For piles in sand and normally-loaded clay, the stiffness factor is calculated using Equation 6:

$$\mathrm{T} = 5\sqrt{\frac{EI}{\eta_h}}\,[\mathrm{m}] \tag{6}$$

where, E is the Young's modulus of the pile material (MN/m^2), I is the moment of inertia of the pile cross-section (m^4), η_h is the modulus of the subgrade reaction (MN/m^3).
For the piles in the rock, the stiffness factor is calculated using Equation 7:

$$\mathrm{R} = 4\sqrt{\frac{EI}{KB}}\,[\mathrm{m}] \tag{7}$$

where, $K = 0{,}3k_1/1{,}5B$, k_1 is the modulus of the subgrade reaction in MN/m^3, B is the width of the pile shaft (diameter in case of circular piles) in m.
The soil subgrade reaction was extracted according to the soil conditions provided in IS 2911 [13]. Based on the above background, the stiffness factor was estimated for fixed-head piles. Subsequently, the point of fixity was determined from the graph using either L1/R or L1/T. The adopted modulus for the subgrade reaction and the fixity values are listed in Table 4.

Table 4. Soil subgrade reaction and fixity

Description	**Pile top CD** (m)	**Dredge level CD** (m)	**Soil Subgrade** (kN/m^3)			**E of pile** (N/mm^2)	**Virtual Fixity in Pile Dia**		
			Sand	**Clay**	**Rock**		**Sand**	**Clay**	**Rock**
Gird-A	5	-22,11	3848	8500	24000	31623	6D	5D	4D
Gird-B	5	-22,11	3848	8500	24000	31623	6D	5D	4D
Gird-C	5	-22,11	3848	8500	24000	31623	6D	5D	4D
Gird-D	5	-22,11	3848	8500	24000	31623	6D	5D	4D
Gird-E	5	-22,11	3848	8500	24000	31623	6D	5D	4D

In the theoretical approach, the bending moment and deflection are determined using Equations 8 and 9, as specified in IS 2911 for fixed-head piles.

$$y = \frac{H(e + z_f)}{12EI}10^3 \tag{8}$$

$$MF = \frac{H(e + z_f)}{2} \tag{9}$$

where y is the deflection of the pile head (mm), H is the lateral load (kN), e is the cantilever length above the ground/bed to the point of load application (m), z_f is the depth to the point of fixity (m), E is the Young's modulus of the pile material in kN/m^2, and I is the moment of inertia of the pile cross-section (m^4).
The horizontal force was obtained from the abovementioned load combinations by considering 1/3rd of the berthing force acting on the 2D frame structure consisting of five rows of piles plus wave and current forces. The average horizontal force on each pile was 255 kN, which was considered in the analysis. For the Fixity method, the IS approach of virtual fixity levels was used to create three fixity models according to the virtual fixity levels in STAAD Pro. The bending moment, shear force, and deflection were obtained from the analyses. The Fixity model is shown in Figure 2.

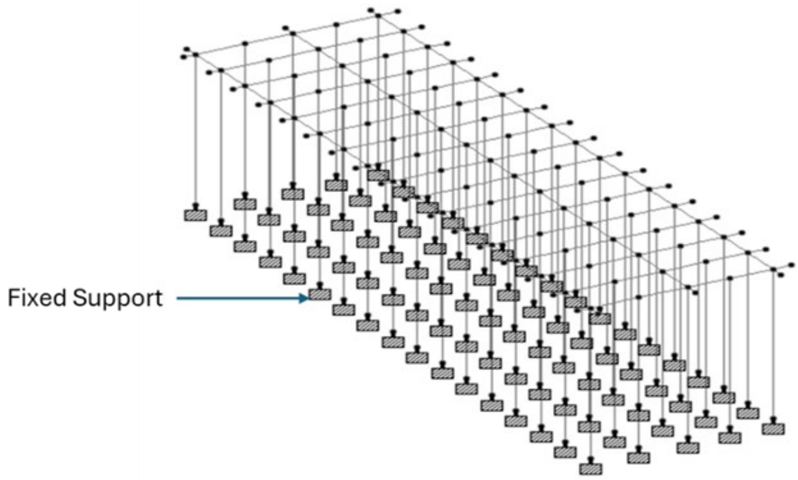

Figure 2. Fixity model

4.2 Linear analysis

A soil-structure interaction linear analysis was performed using springs to represent the soil. The spring stiffness was calculated based on the following procedure for sand, clay, and rock. The modulus of the subgrade reaction (k_s) was calculated using the Vesic (Bowels, 1974) equation as in Equation 10 [13].

$$k_s{}' = 1{,}3\sqrt[12]{\frac{E_s B^4}{E_p I_p}}\left(\frac{E_s}{1-\mu^2}\right) \tag{10}$$

where, E_s and E_p are the modulus of the soil and pile, respectively, in consistent units, B and I_p are the diameter and moment of inertia of the pile, respectively, and μ^2 is the Poisson's ratio of the soil (0,2-0,4).
The parameter k_s was obtained from k_s' as in Equation 11:

$$k_s = \frac{k_s{}'}{B} \tag{11}$$

The spring stiffness was calculated based on the Newmark (1942) distribution, as shown in Equations 12, 13 and 14 [6]. First spring stiffness:

$$k_1 = \frac{BL}{24}\left(7k_{s_{(1)}} + 6k_{s_{(2)}} - k_{s_{(3)}}\right) \tag{12}$$

Intermediate spring stiffness:

$$k_i = \frac{BL}{12}\left(k_{s_{(i-1)}} + 10k_{s_{(i)}} + k_{s_{(i+1)}}\right) \tag{13}$$

Last spring stiffness:

$$k_n = \frac{BL}{24}\left(7k_{s_{(n)}} + 6k_{s_{(n-1)}} - k_{s_{(n-2)}}\right) \tag{14}$$

where, L is the segment length. Each segment of the pile was represented by springs and the segment length was chosen to maintain a ratio of 1 between the segment length and pile diameter (L/d). The soil stiffness was determined for each soil layer, and is presented with the corresponding elevation levels in Table 5. The linear model is illustrated in Figure 3.

Table 5. Linear spring values

S. No.	Level with respect to CD (m)	Pile dia (m)	Sand	Clay	Rock
			Spring value (kN/m)		
1	−22,86	1,5	7201	62426	3296101
2	−24,36	1,5	14402	124852	6592202
3	−25,86	1,5	14402	124852	6592202
4	−27,36	1,5	15129	124852	6592202
5	−28,86	1,5	22390	124852	6592202
6	−30,36	1,5	23116	124852	6592202
7	−31,86	1,5	23116	124852	6592202
8	−33,36	1,5	23116	124852	6592202
9	−34,86	1,5	23116	124852	6592202
10	−36,36	1,5	23116	124852	6592202
11	−37,86	1,5	23116	124852	6592202
12	−39,36	1,5	23116	124852	6592202
13	−40,86	1,5	23116	124852	6592202
14	−41,60	1,5	5779	31213	3296101

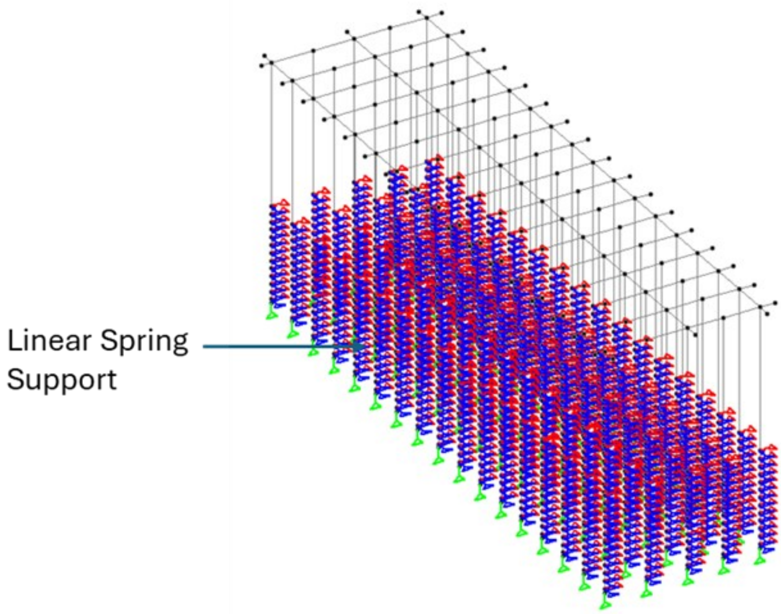

Figure 3. Linear-soil interaction model

4.3 Non-linear analysis

The p-y technique is widely used in the design of laterally loaded piles [20]. This technique uses several separate non-linear springs to replace soil reactions. The relationship between the soil reaction and pile deflection at various positions along the pile length is shown by p-y curves that indicate the non-linear behaviour of the soil. The p-y curve was generated using L pile software, considering the specified soil parameters for sand, clay, and rock. The method developed by Reese et al. (1974) was employed to compute the p-y curves in sand, and the stiff clay method was used for clay, and the weak rock method was used for rock. The resulting p–y values are listed in Table 6. The p-y model is shown in Figure 4.

Table 6. Typical P-Y values

Sand		Clay		Rock	
y (mm)	**p** (kN)	**y** (mm)	**p** (kN)	**y** (mm)	**p** (kN)
0,377	67	0,005	119	0,024	2955
2,615	199	0,076	238	0,263	5402
4,854	282	0,384	358	0,503	6352
7,092	349	1,214	477	0,742	7002
9,331	407	2,963	596	0,982	7509
11,569	460	6,144	715	1,221	7930
13,808	508	11,383	834	2,419	9407
16,046	553	19,418	953	3,616	10403
18,285	595	31,104	1073	4,814	11174
20,523	635	47,407	1192	6,012	11812
22,762	673	69,409	1311	7,209	12361
25,000	710	98,304	1430	8,407	12845
40,625	960	135,400	1549	9,605	13280
56,250	1211	182,120	1668	10,802	13676
67,500	1211	240,000	1788	12,000	14040
78,750	1211	300,000	1788	15,000	14040

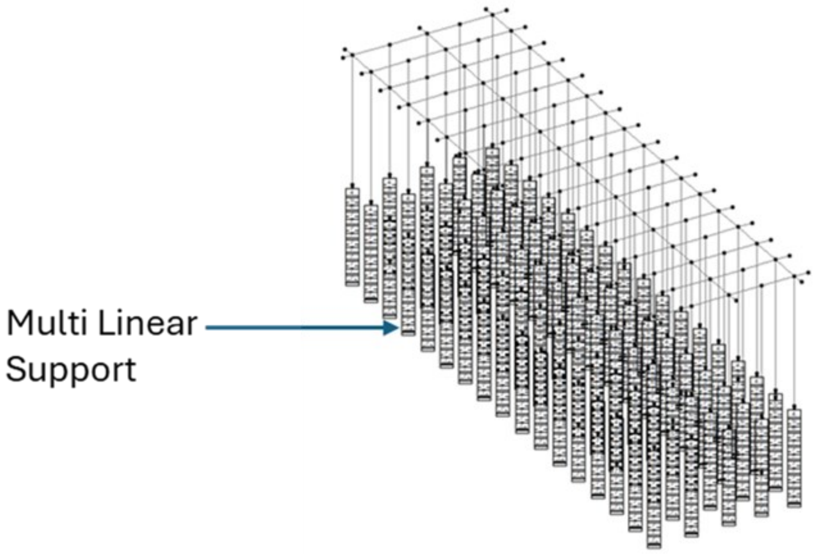

Figure 4. Non-linear P-Y model

5 Results and discussion

The results obtained from the IS approach, fixity method, linear analysis, and non-linear analysis under appropriate soil conditions [21; 22] were compared. From the IS approach, the deflection, bending moment and shear force were calculated in accordance with IS 2911 [15]. The major lateral load was caused by the berthing of the vessel [23] and lateral forces induced by waves and currents simultaneously. With this background, a 2D analysis was carried out, and the results are listed in Table 7. IS analysis was further compared with the other three analyses.

The comparison between the IS approach and analyses utilising the fixity, linear, and non-linear methodologies in assessing deflection, shear force at the top and bottom, and bending moment at the top and bottom of the berthing structure situated in sand at Chennai port is shown in Figure 5a), 5b), 5c) and 5e), respectively. In terms of deflection, there is a reduction of 16 % for fixity and 20 % in both linear and non-linear analyses compared to the IS approach. The shear force at the top decreases by 35%, 35%, and 37%, whereas that at the bottom decreases by 7,0 %, 8,5 %, and 7,0 % using the fixity method, linear analysis, and non-linear analysis, respectively. The bending moment at the top decreases by 20 %, 23 %, and 23 %, whereas that at the bottom decreases by 8 %, 45 %, and 42 % using the fixity method, linear analysis, and non-linear analysis, respectively.

The comparison between the IS approach and analyses utilising fixity, linear, and non-linear methodologies to evaluate the deflection, shear force at the top and bottom, and bending moment at the top and bottom of the berthing structure situated in clay at Cochin port are shown in Figure 6a), 6b), 6c), and 6e), respectively. In terms of deflection, there is a reduction of 16 % for the fixity method and 32% for both the linear and non-linear analyses compared with the IS approach. The shear force at the top decreases by 35 %, 33 %, and 37 %, whereas that at the bottom decreases by 6%, 4%, and 8% using the fixity method, linear analysis, and non-linear analysis, respectively. The bending moment at the top decreases by 20 %, 24 %, and 26 %, whereas that at the bottom decreases by 7 %, 38 %, and 40 % using the fixity method, linear analysis, and non-linear analysis, respectively.

A comparison of the deflection, shear force at the top and bottom, and bending moment at the top and bottom of the berthing structure situated in rocks at Bhavanapadu Port are shown in Figure 7a), 7b), 7c), and 7e), respectively, between the IS approach and different models. In terms of deflection, there is a reduction of 16 % for fixity and 32 % for both linear and non-linear analyses compared with the IS approach. The shear force at the top decreases by 34 %, 29 %, and 30 %, whereas that at the bottom decreases by 5,0 %, 2,0 %, and 2,5 % using the fixity method, linear analysis, and non-linear analysis, respectively. The bending moment at the top decreases by 19%, 26%, and 26%, whereas that at the bottom decreases by 6 %, 24 %, and 26 % using the fixity method, linear analysis, and non-linear analysis, respectively.

Table 7. Bending moment, shear force and deflection results of the IS 2911 approach

<table>
<tr><th rowspan="3">Pile Dia (1,5 m)</th><th colspan="5">Chennai Port (Sand)</th><th colspan="5">Cochin Port (Clay)</th><th colspan="5">Bhavanapadu Port (Rock)</th></tr>
<tr><th colspan="2">Shear (kN)</th><th colspan="2">BM (kNm)</th><th rowspan="2">Deflection (mm)</th><th colspan="2">Shear (kN)</th><th colspan="2">BM (kNm)</th><th rowspan="2">Deflection (mm)</th><th colspan="2">Shear (kN)</th><th colspan="2">BM (kNm)</th><th rowspan="2">Deflection (mm)</th></tr>
<tr><th>T</th><th>B</th><th>T</th><th>B</th><th>T</th><th>B</th><th>T</th><th>B</th><th>T</th><th>B</th><th>T</th><th>B</th></tr>
<tr><td>Gird-A</td><td colspan="2">255</td><td colspan="2">4369</td><td>127</td><td colspan="2">255</td><td colspan="2">4188</td><td>112</td><td colspan="2">255</td><td colspan="2">4006</td><td>98</td></tr>
<tr><td>Gird-B</td><td colspan="2">255</td><td colspan="2">4369</td><td>127</td><td colspan="2">255</td><td colspan="2">4188</td><td>112</td><td colspan="2">255</td><td colspan="2">4006</td><td>98</td></tr>
<tr><td>Gird-C</td><td colspan="2">255</td><td colspan="2">4369</td><td>127</td><td colspan="2">255</td><td colspan="2">4188</td><td>112</td><td colspan="2">255</td><td colspan="2">4006</td><td>98</td></tr>
<tr><td>Gird-D</td><td colspan="2">255</td><td colspan="2">4369</td><td>127</td><td colspan="2">255</td><td colspan="2">4188</td><td>112</td><td colspan="2">255</td><td colspan="2">4006</td><td>98</td></tr>
<tr><td>Gird-E</td><td colspan="2">255</td><td colspan="2">4369</td><td>127</td><td colspan="2">255</td><td colspan="2">4188</td><td>112</td><td colspan="2">255</td><td colspan="2">4006</td><td>98</td></tr>
</table>

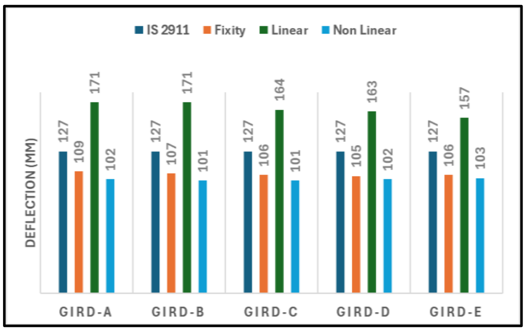

a) Comparison of deflection (sand)

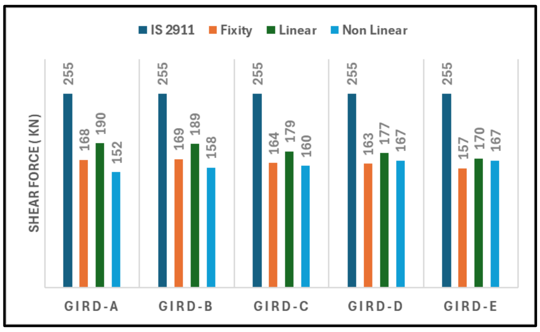

b) Comparison of shear force at the top (sand)

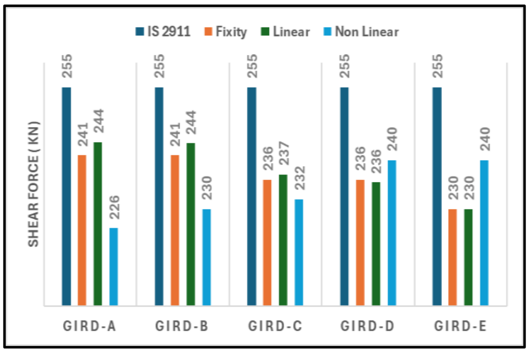

c) Comparison of shear force at the bottom (sand)

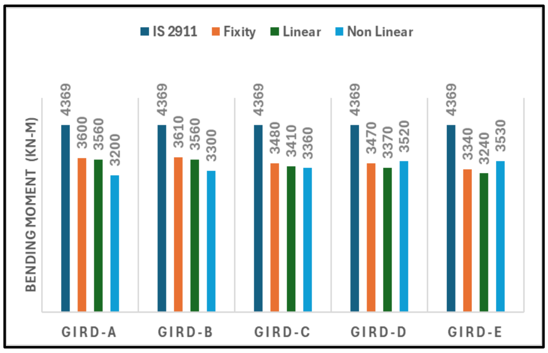

d) Comparison of bending moment at the top (sand)

e) Comparison of bending moment at the bottom (sand)

Figure 5. Comparison of results for the berthing structure in sand

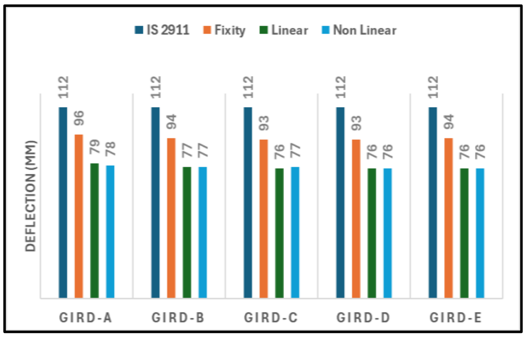

a) Comparison of deflection (clay)

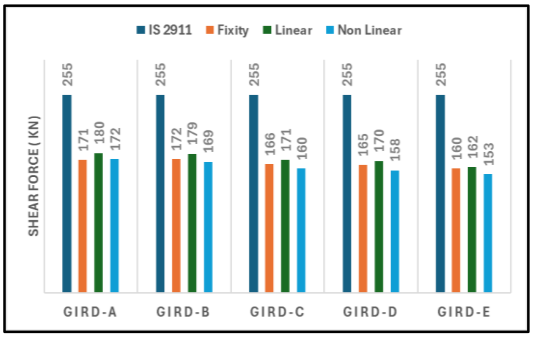

b) Comparison of shear force at the top (clay)

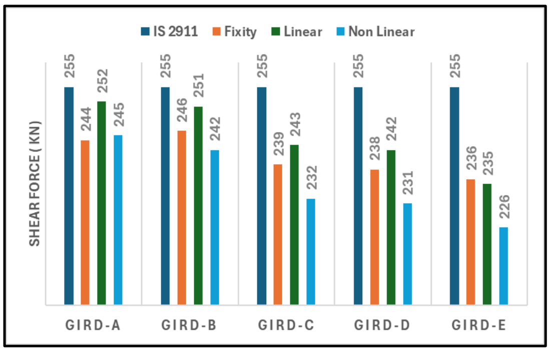

c) Comparison of shear force at the bottom (clay)

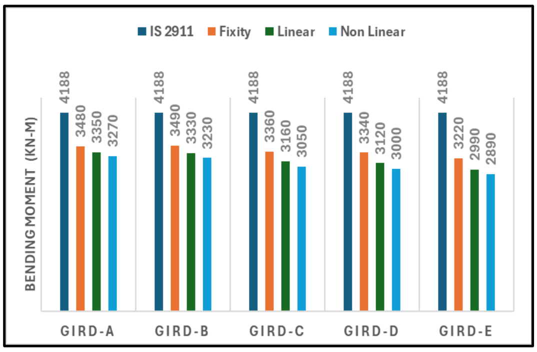

d) Comparison of bending moment at the top (clay)

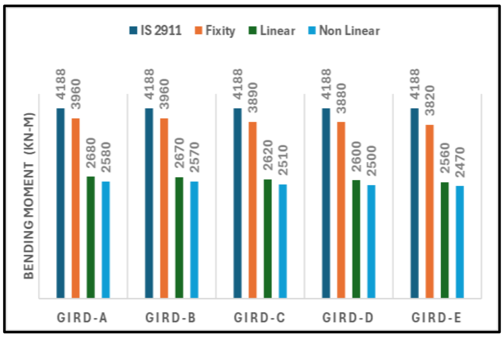

e) Comparison of bending moment at the bottom (clay).

Figure 6. Comparison of results for the berthing structure in clay

a) Comparison of deflection (rock)

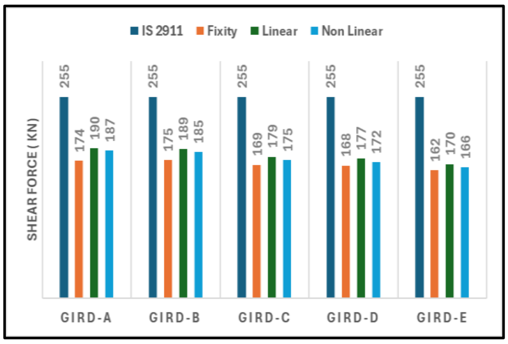

b) Comparison of shear force at the top (rock)

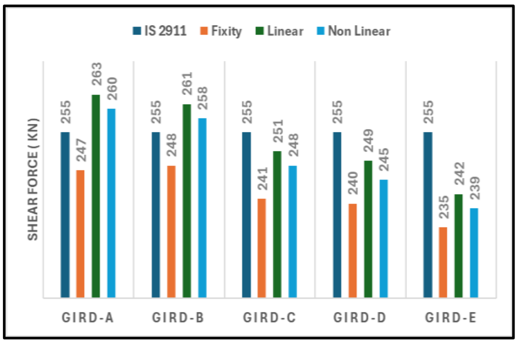

c) Comparison of shear force at the bottom (rock)

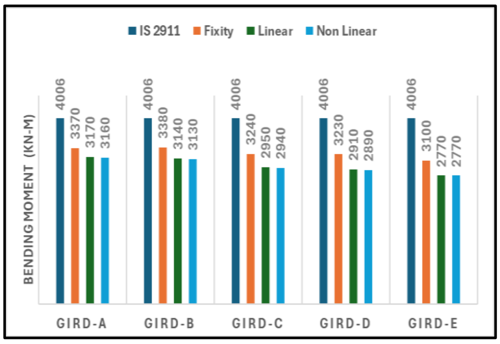

d) Comparison of bending moment at the top (rock)

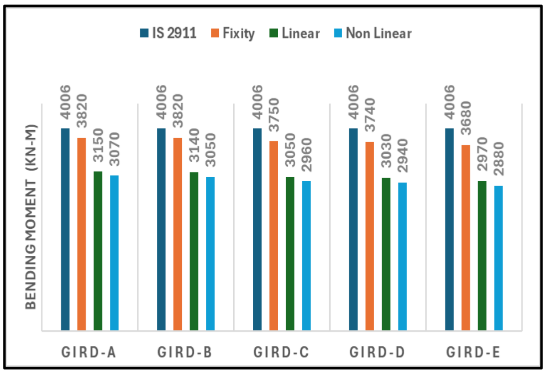

e) Comparison of bending moment at the bottom (rock)

Figure 7. Comparison of results for the berthing structure in rock

6 Conclusion

In this study, analysis techniques such as the IS approach, Fixity method, linear analysis, and non-linear analysis were conducted to optimise the costs of construction materials, specifically for establishing the bill of quantities at the project's outset, particularly concerning berthing substructures in deep-draft environments. The following conclusions were drawn:

- Linear and non-linear analyses proved to be more cost-effective than the IS and soil fixity approaches.
- Specifically for sand, the bottom bending moment was reduced by approximately 30 %, with a 10 % reduction at the top.
- For clay, a reduction of 25 % at the bottom and 10 % at the top were achieved.
- For rocks, both the bottom and top bending moments were reduced by 10 %.

Project planners and engineers can achieve substantial reductions in bending moments by utilising the IS approach during the initial establishment of a bill of quantities for berthing substructures. This eliminates the need for time-consuming linear and non-linear analyses. Thus, this approach can enable significant material cost savings, while ensuring adherence to industry standards, particularly those tailored to specific soil types such as sand, clay, and rock.

This study prioritises simplicity (IS approach) over accuracy, potentially overlooking complex soil behaviours and dynamic loads. It also mainly focuses on the bending moments and ignores other critical structural responses. Future research should include varied and mixed soil types, assess long-term lifecycle costs, and validate the findings through real-world case studies.

References

[1] Bureau of Indian Standards. IS 4651 (Part-III): 2020. *Code of Practice for Planning and Design of Ports and Harbors – Loadings, 2nd rev*. New Delhi: BIS; 2020.

[2] Jayasree, P. K.; Arun, K. V.; Oormila, R.; Sreelakshmi, H. Lateral Load Capacity of Piles: A Comparative Study Between Indian Standards and Theoretical Approach. *Journal of The Institution of Engineers (India): Series A*, 2018, 99 (3), pp. 587-593. https://doi.org/10.1007/s40030-018-0306-7

[3] Santosh Kumar, B.; Ashok Kumar, S. Analysis and design of dock berth structure. *IRJET*, 2016, 2 (3), pp. 8-16.

[4] Priyanka, K.; Neela, V. B. Assessment of structural behaviour of jetty under marine loads and its design for berthing of vessels. *IJSRD - International Journal for Scientific Research & Development*, 2019, 7 (10), pp. 438-441.

[5] Chopra, H. B.; Patel, P. G. Application of forces acting on jetty structure. *IJSTE - International Journal of Science Technology & Engineering*, 2015, 1 (11), pp. 83-91.

[6] Rajkumar, M.; Satyanarayana, G. V. Structural system evaluation of jetties. *IJSTE - International Journal of Science Technology & Engineering*, 2016, 3 (8), pp. 153-160.

[7] Chaudhari, Y.; Datta, D.; Joshi, V. Estimation of marine loads on jetty structure. *Journal of Civil Engineering and Environmental Technology*, 2016, 3 (5), pp. 440-446.

[8] Ministry of Shipping, Indian Ports Association. Master Plan for Chennai Port. Accessed: September 29, 2025. Available at: https://sagarmala.gov.in/sites/default/files/Final_Master_Plan_ChPT.pdf

[9] Ministry of Shipping, Indian Ports Association. Master Plan for Cochin Port. Accessed: September 29, 2025. Available at: https://sagarmala.gov.in/sites/default/files/Final_Master%20_Plan_Cochin.pdf

[10] Cochin Port Trust. Re-construction of South Coal Berth at Cochin Port on EPC Contract Basis, Geotechnical Investigation Report, Volume IV. Accessed: September 29, 2025. Available at: https://www.cochinport.gov.in/sites/default/files/2020-08/Addendum%20-%20Corrigendum%20No.1--.pdf

[11] Indian Ports Association. Consultancy services for pre-feasibility of Greenfield Port at Bhavanapadu in Srikakulam District, Andhra Pradesh. Accessed: September 29, 2025. Available at: https://environmentclearance.nic.in

[12] Bureau of Indian Standards. IS 1893 (Part-I): 2002. *Criteria for Earthquake Resistant Design of Structures – General Provisions and Buildings*. New Delhi: BIS; 2002.

[13] Bowles, J. E. Foundation Analysis and Design. 5th Edition, New York: McGraw-Hill, 1997.

[14] Bureau of Indian Standards. IS 4651 (Part-V): 1997. *Code of Practice for Planning and Design of Ports and Harbors – Layout and Functional Requirements, 3rd rev*. New Delhi: BIS; 1997.

[15] Bureau of Indian Standards. IS 2911 (Part I/Sec II): 2010. *Design and Construction of Pile Foundations*. New Delhi: BIS; 2010.

[16] Bureau of Indian Standards. IS 4651 (Part-IV): 2019. *Code of Practice for Planning and Design of Ports and Harbors – General Design Considerations, 3rd rev*. New Delhi: BIS; 2019.

[17] Bureau of Indian Standards. IS 875 (Part-III): 2015. *Code of Practice for Design Loads for Buildings and Structures – Wind Loads*. New Delhi: BIS; 2015.

[18] Bureau of Indian Standards. IS 875 (Part-I): 2008. *Code of Practice for Design Loads (Other Than Earthquake) for Buildings and Structures – Dead Loads – Unit Weights of Building Materials and Stored Material*. New Delhi: BIS; 2008.

[19] Atiq, M. S.; Shajib, A. K. J.; Hoque, K. N. Analysis of marine fender systems minimizing the impact of collision damage. In: *Proceedings of the 13th International Conference on Marine Technology (MARTEC 2022)*. December 21-22, 2022, Dhaka, Bangladesh, Elsevier; 2023, pp. 76(1-9). https://doi.org/10.2139/ssrn.4445128

[20] Ensoft, Inc. A program for the analysis of deep foundations under lateral loading (LPILE v2022 Technical Manual). Accessed: September 29, 2025. Available at: https://studylib.net/doc/26047618/lpile-2022-user-manual

[21] Bureau of Indian Standards. IS 4651 (Part-I): 2020. *Code of Practice for Planning and Design of Ports and Harbors – Site Investigation, 2nd rev*. New Delhi: BIS; 2020.

[22] Bureau of Indian Standards. IS 4651 (Part-II): 2020. *Code of Practice for Planning and Design of Ports and Harbors – Geotechnical Engineering, 2nd rev*. New Delhi: BIS; 2020.

[23] Belagavi, V.; Rugi, K. B. Analysis and design of berthing structure. *International Research Journal of Engineering and Technology (IRJET)*, 2019, 06 (11), pp. 1623-1629.